Visual Sensing and Image Processing for Error Detection in Laser Metal Wire Deposition

A. I. Adediran*, A. Nycz*, A. Thornton†, L.J. Love*

*Energy & Transportation Science Division, National Transportation Research Center, Oak Ridge National Laboratory, Knoxville, TN 37830
†Additive Manufacturing Technology Center, GKN Aerospace - St. Louis Hazelwood, MO 63042

Abstract

Laser metal deposition with wire (LMD-w) involves feeding metal wire through a nozzle and melting the wire with a high-power laser. With efficient process control, i.e. sensing, processing, and feedback correction of errors, the technology has the potential to change the course of manufacturing. However, the limitation most often encountered in LMD is the difficulty in controlling the process. Monitoring and control of metal additive manufacturing processes has been mostly researched on powder-based systems and has not been extensively investigated on metal wire feed systems. This work proposes a method for detecting discontinuities in a deposited layer in the LMD-w process via optical inspection and processing of images obtained from a high-resolution camera. The aim is to develop an effective sensing module that automatically detects irregularities in each layer before proceeding to subsequent layers, which will reduce part porosity and improve inter-layer bond integrity.

Introduction and Background

Laser metal deposition is an additive manufacturing technique for building metal parts directly from a computer-aided design (CAD) drawing. The process involves using a high-energy laser beam to melt metal wire into beads onto a substrate side by side and layer by layer. In many setups, robotic controls are used to manipulate the laser beam-wire nozzle assembly and the melt pool along a 3D path. The melt pool then solidifies to form specific geometries as defined by the original CAD model. A schematic representation of the LMD-w process is shown in Figure 1.

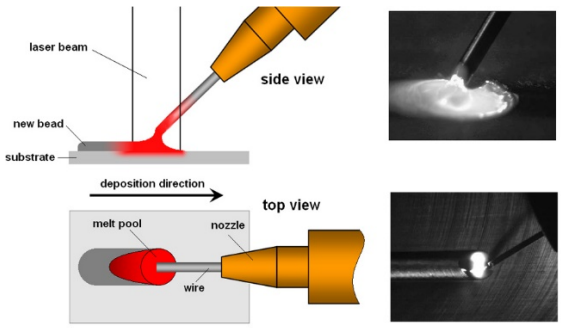

Fig. 1. A schematic diagram of the LMD-w process [1]

Laser metal wire deposition is largely being applied in the aerospace industry, where the focus is on manufacturing large, major structural components for aircraft, such as spars, bulkheads, and frames that are traditionally fabricated from machined forging or plate material. Figure 2 shows some major aircraft parts made from Titanium. In aircraft production, the use of laser metal deposition has two main benefits – cost and efficiency. Typically, large Titanium forgings have significantly long lead times, and the machining process can be highly energy and material inefficient. The average buy-to-fly ratio (BTF) in the fabrication of aircraft parts using traditional methods of subtractive manufacturing is 10:1. A BTF ratio of 10:1 means that about 10 pounds of stock material is required to make a 1-pound part, with 90 percent material discarded as scrap. BTF ratios even greater than 20:1 are a common occurrence[1]. In contrast, additive manufacturing produces very little waste and reduces the cost of machining a block of material down to desired shape. LMD is cited as saving 90 percent of raw material at less than 10 percent of the cost of the same part produced through subtractive manufacturing. [2-4] Efficient control could help reduce lead time by as much as 80 percent, enable fabrication of parts having intricate shapes that maintain strength while significantly cutting the weight of the part by up to 40 percent.[5]

Fig. 2. Sample aircraft parts made of Titanium. (a) Forged landing gear [6] (b) 5m^2 3D-printed Titanium alloy load-bearing frame [7]

Prior Art and Research Motivation

Several studies have been conducted on monitoring and control of metal additive manufacturing processes. Examples include monitoring and process control using cameras [8-10], closed-loop height control using photodiodes [11-14], powder flow control based on motion system speed profile [15], and temperature measurements using pyrometers [16-18]. However, these works focus on powder-based systems (powder bed and blown powder). The subject has not been extensively investigated on metal wire feed systems, and the results from powder-based systems cannot be simply transferred to wire-based deposition systems since the two processes are dissimilar in many ways.[19, 20] LMD-w has the advantages of higher deposition rates, wider availability of wire products, and cheaper feedstock over powder counterparts[21]. Thus, it is worthwhile to investigate process control for laser metal wire processes in depth.

Despite the interesting possibilities for laser additive manufacturing, there are challenges in terms of qualification and certification. Safety concerns on the accuracy of the AM process, how printed products will perform over time, and the consistency of their quality keeps the additive process at a lower maturity level compared to conventional subtractive processes.[22] The U.S. Air Force Research Laboratory (AFRL/ML) and the Metals Affordability Initiative (MAI) have identified that from a purely technical standpoint, an additive manufacturing technology cannot be considered for the manufacture of aircraft components unless the process is stable and controlled, and the resulting mechanical properties are well characterized and sufficiently invariable. [23] On-line monitoring and automatic error detection is therefore necessary to ensure process stability and material integrity.

Error Definition

In wire-fed systems, the geometry of each bead is a vital process variable that can provide valuable information about the properties of the final manufactured part, such as dimensional accuracy, surface finish, and mechanical properties. [24] Measurements obtained from monitoring the bead geometries can thus be used to control other parameters that drive the process, such as robot travel speed, laser power, wire speed, etc. to achieve better part quality.

The goal of the monitoring approach described in this paper is to be able to view the melt pool in-process and to accurately detect deviations in the width of the pool along the bead. The ideal outcome in the laser wire deposition process is a perfectly straight bead profile. That is, each bead has straight-line edges and maintains a set horizontal width at a constant value throughout the travel of the manipulator while executing a layer. Deviations from the target bead widths are then flagged for subsequent use in determining the necessary corrective actions to restore the width to desired values.

An “error”, as used in this writing, is a distance deviation (in the x-direction in Figures 3 and 4) from a reference point. An error refers to a positive or negative difference between the measured width of a bead on any layer ***n*** and a reference width value set to be equal or relative to the ideal width of that layer. A positive error, or a ‘*neck*’, refers to an indentation in the profile, while a negative error, or a *‘bulge’*, refers to an outward protrusion in the profile.

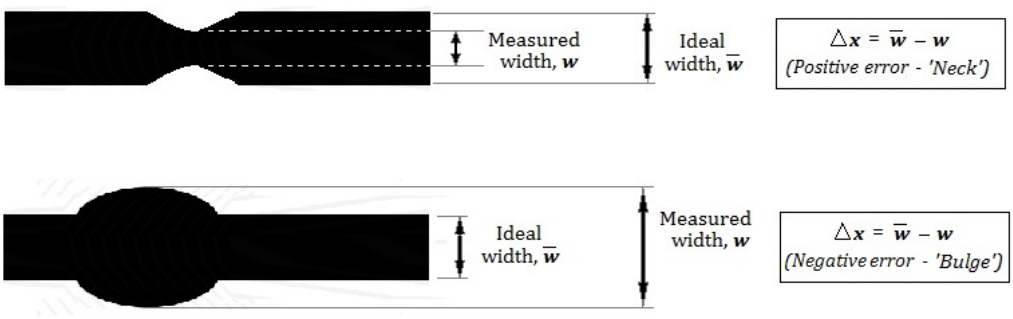

Fig. 3. Schematic representation of a positive and a negative error

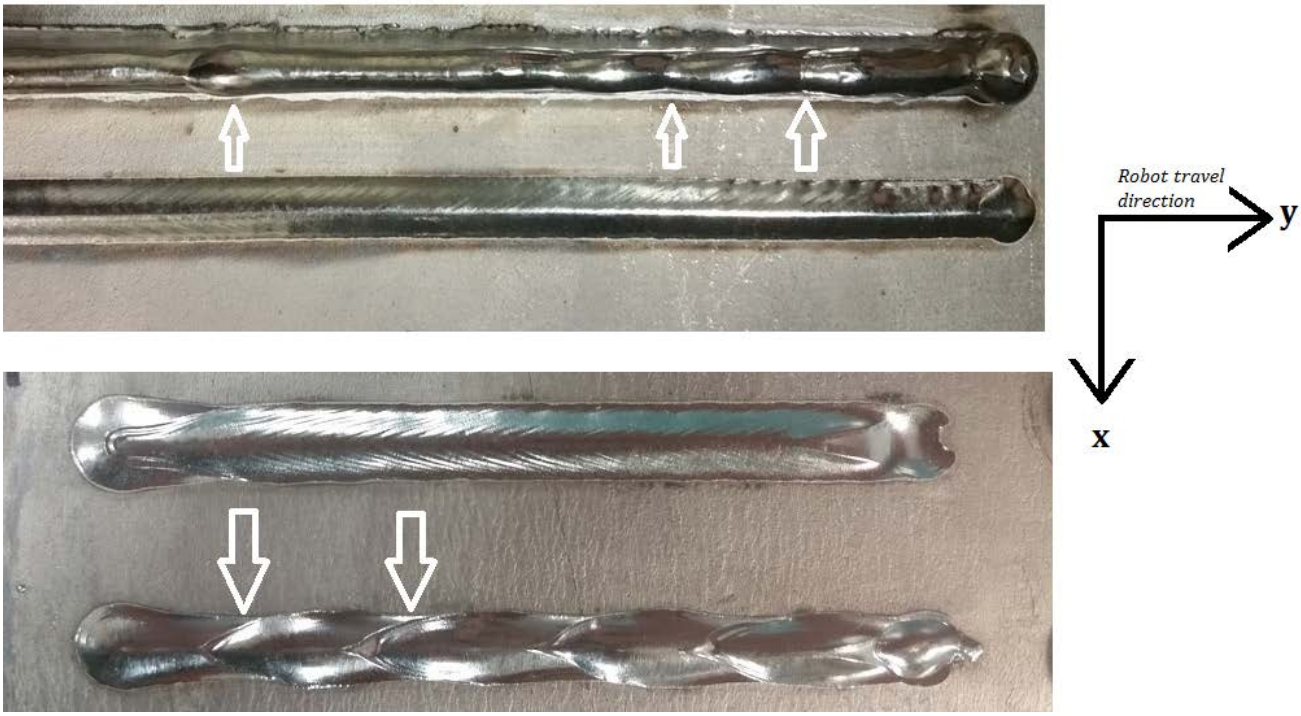

Fig. 4. Discontinuities in the x-y plane

Bead Width Monitoring Via Image Processing

Due to the extreme brightness of the melt zone in the LMD process, visualizing the melt pool is done via a high-definition CMOS-based camera equipped with cascaded neutral density filters to significantly reduce the intensity of the melt pool. The setup is shown in Figure 5.

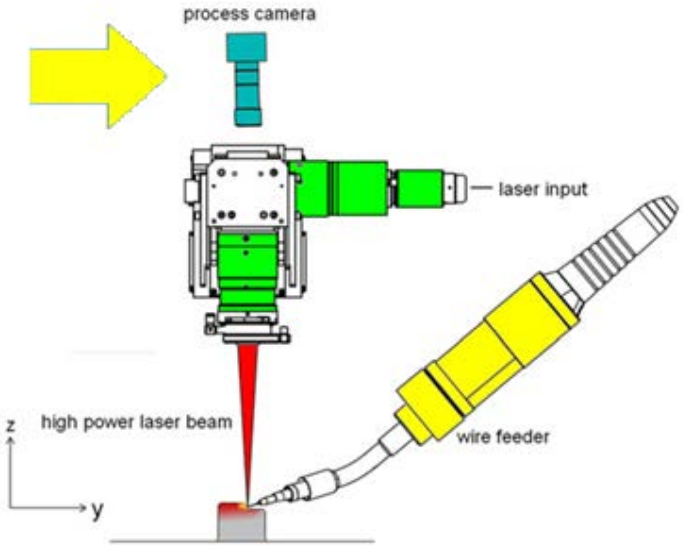

Fig. 5. Apparatus setup for melt pool imaging

Optical images are extracted from recorded videos of each bead in the form of image frames. The processing of extracted frames to identify bead geometries is done in five steps: i)

Region of Interest Extraction, ii) Binarization, iii) Noise extraction, iv) Geometry measurement, and v) Data Conversion & Logging

i. Region of Interest (ROI) Extraction – The first stage of the process allows the operator to interactively define a portion of the entire frame on which filtering and further processing will be done. This is necessary because the only useful visual information is the melt pool region, while the rest of the frame is redundant. This exclusion helps to save computing power and processing time.

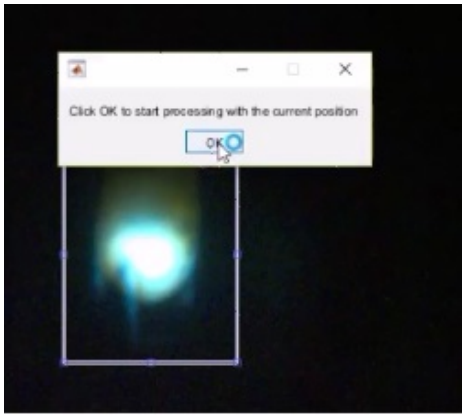

Fig. 6. Interactive ROI Extraction

ii. Binarization – A typical frame obtained from the ROI extraction is essentially an RGB (Red-Green-Blue) image or true color image. An RGB frame is stored as an m-by-n-by-3 data array of pixel defining red, green, and blue color components for each individual pixel. The true color image is converted to a grayscale image in which the value of each pixel carries only intensity information. The grayscale image entirely contains varying shades of gray with black being the weakest intensity and white being the strongest. The pixel intensity values are then compared against a set threshold that sets pixels within the range to 1 and all others to 0, as shown in Figure 7 using a sample threshold of 100. The resulting image is an array of 0s and 1s, where a 0 is a black pixel and a 1 is a white pixel. With this process, the boundary of the melt pool region is extracted.

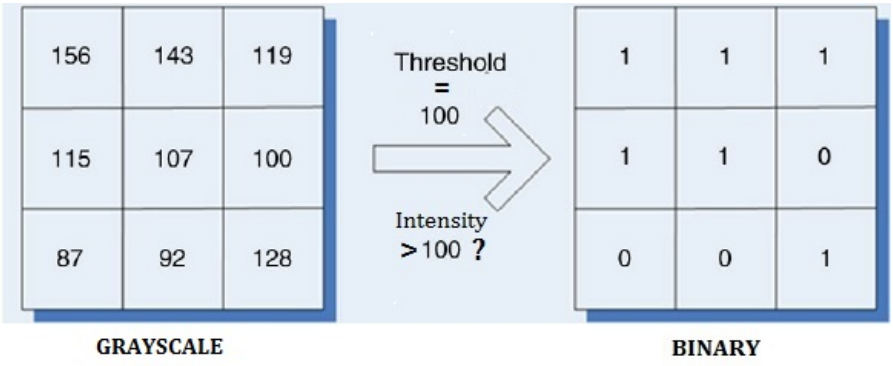

Fig. 7. Schematic representation of the binarization process

iii. Noise extraction – Occasional unwanted noise in acquired images due to sparks, plumes, or some other emission is a common occurrence in the LMD process, and noise needs to be filtered out to prevent false interpretation of image data by the algorithm. Noise is identified in the binary image as small clusters of white pixels or '1' values in the array that are significantly smaller in area in comparison to with the actual melt pool, as depicted in the bottom-right image of Figure 8. The filtration is done by setting all such clusters to '0', essentially turning them to black.

iv. Geometry measurement – In this process, the needed measurements of bead width are extracted, i.e. the horizontal distance between the edges of the melt pool. The width of the bead is measured as the width of the smallest rectangle binding the image of the melt pool as shown in Figure 8.

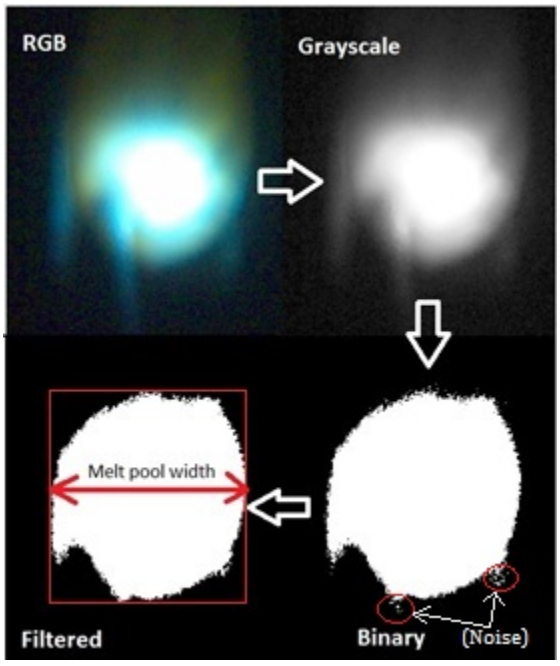

Fig. 8. Image processing steps applied to a typical melt pool image

v. Data Conversion & Logging – Raw geometry measurement data is initially presented in pixel units. The conversion to distance units is done at this stage. The converted values are then compared with the target value of the melt pool width from which error ('neck' and 'bulge') points are logged.

User-Interactive Thresholding

When monitoring the melt pool in the LMD process, determining the exact bounding region of the melt pool is sometimes a challenge because each build job mostly features different parameters and process disturbances. Even under identical process conditions, changes in camera settings such as focus and filtering could occur. These factors may make the melt pool appear different from build to build. The user-interactive thresholding concept is introduced to allow pre-build calibration to teach the monitoring system to correctly identify the melt pool prior to the start of the actual build process. To implement this, a test bead is run and the calibration is done via visual judgement of the operator, i.e. the threshold, as discussed in the binarization stage above, is set by interactively tuning intensity parameters and visually observing the response until a satisfactory match between visually observed and computer-detected melt pool region is achieved. It should be noted that for best results, a suitable camera capable of providing clearly discernable images of the melt pool is necessary. Several studies have already been conducted on visualization of melt pools in laser deposition and welding processes. [25-30] Figure 9 shows images in the pre-build calibration. In (a), the threshold is set too low resulting in a detected 'pool' far out from the actual melt pool. In (b), the threshold is set too high and does not capture all of the melt pool. Figure 9(c) shows a satisfactory setting.

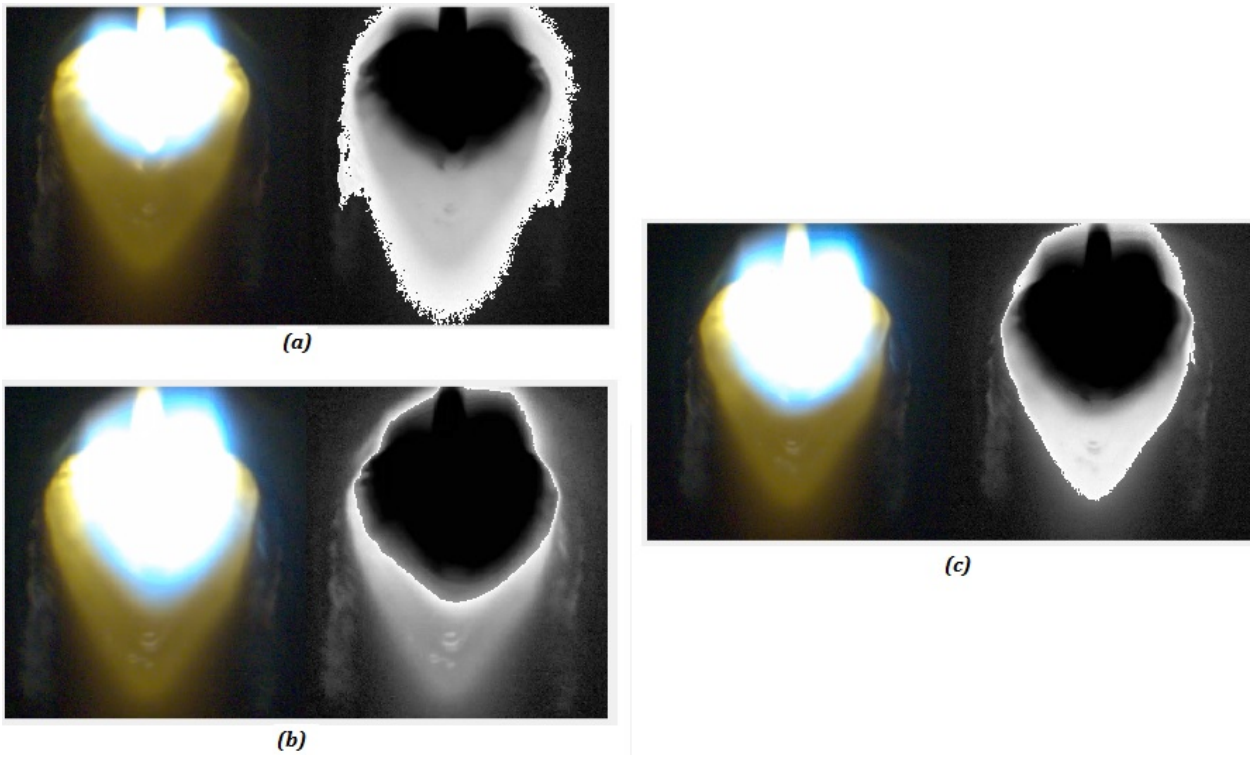

Fig. 9 Pre-build calibration

Results and Discussion

The table in Figure 10 shows experimental bead width error measurements for a 150mm bead, which were logged from the image processing system. In this instance, a tolerance of ±0.5mm was used in flagging an error.

Type	*e*-Value	DistanceFromOrigin (in mm)
'Bulge'	1.2632	11.6733
'Bulge'	1.2632	12.3407
'Bulge'	1.2105	13.0080
'Bulge'	1.3158	13.6753
'Bulge'	1.3158	14.3427
'Neck'	0.5789	64.3927
'Neck'	0.5789	65.0601
'Neck'	0.5789	65.7274
'Neck'	0.5789	66.3947
'Neck'	0.5789	67.0621
'Neck'	0.5789	67.7294
'Neck'	0.5789	68.3967
'Bulge'	1.1579	123.1181
'Bulge'	1.1579	123.7855
'Bulge'	1.1579	124.4528
'Bulge'	1.1579	125.1201
'Bulge'	1.1579	125.7875
'Bulge'	1.1579	126.4548
'Bulge'	1.1579	127.1221
'Bulge'	0.7368	146.4748
'Bulge'	0.7368	147.1421

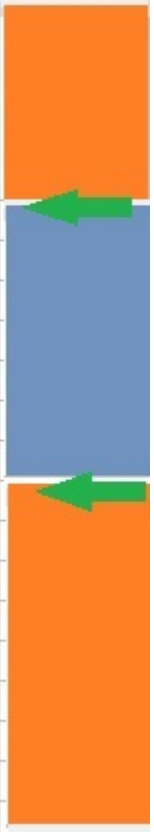

Fig. 10 Bead width measurements

From the results, it can be deduced that the bead profile has 3 erroneous sections: a widening of ~1.3mm a short distance from the start of the bead, a slight narrowing by ~0.6mm beginning from ~65mm into the bead running for about 5mm, and another widening toward the end of the bead from ~123mm. In-between these sections (indicated by the arrows in Figure 10), the bead remains steady within the tolerance range of the target width, for a distance of ~50mm and ~ 55mm, respectively. These error amounts, or the ***e***-values, are valuable metrics that can be used in developing a closed-loop control system (also known as a feedback control system), which self-adjusts to compensate for the deviations. It has been found from experimental and analytical approaches that robot travel speed and laser power significantly affect the diameter of a weld bead. Higher powers tend to result in wider and flatter beads, while lower powers yield thin, peaky beads. The width of a bead is also found to be a function of speed, decreasing as deposition speed increases.[31] Taking the above error data as feedback signals, these relationships can be used to develop the feedback control system, which automatically computes necessary corrective modifications to the process variables and maintains the bead width at its target value.

Conclusion

A monitoring system for wire-fed laser metal deposition has been developed and evaluated by depositing single beads. The proposed monitoring system features an interactive pre-build calibration of the melt pool region via visual inspection and judgement, enabling the operator to 'teach' the system to correctly identify the melt pool of any build session. The system detects deviations from a target melt pool width and logs error data that can be used in developing a robust automatic error control system through the manipulation of key process variables. It has been found that the bead diameter is significantly dependent on the speed of deposition (i.e. the robot travel speed) and the laser power. Other key process variables worth noting, and possibly inclusion in a robust control system design, are the wire input speed and the nozzle-to-top-surface distance (NTSD). The development of the automatic error control system following these results and relationships will be studied in future work.

Acknowledgments

The work described in this paper was jointly supported by the Manufacturing Systems Research group of the Manufacturing Demonstration Facility, Oak Ridge National Laboratory, GKN Aerospace, and the Bredesen Center for Interdisciplinary Research and Graduate Education, University of Tennessee.

References

1. GKNAerospace. *Large Scale Deposition - Laser Wire*. Available from: http://www.gkngroup.com/additive-manufacturing/processes-applications/GKN-Aerospace/Pages/large-scale-deposition-laser-wire.aspx.
2. OECD, *The Next Production Revolution Implications for Governments and Business: Implications for Governments and Business*. 2017: OECD Publishing.
3. Alec. *China developing world's largest 3D printer, prints 6m metal parts in one piece*. 2014; Available from: http://www.3ders.org/articles/20140207-china-developing-world-largest-3d-printer--prints-6m-metal-parts-in-one-piece.html.
4. Anderson, E., *Additive Manufacturing in China: Aviation and Aerospace Applications (Part 2)*. 2013.
5. Yang, S. *Titanium Alloy 3D Print 2012 China First Invention*. 2013-01-21; Available from: http://www.guancha.cn/shi-yang/2013_01_21_122111.shtml.
6. KobeSteelLTD. *Kobe Steel begins mass production of Titanium forged parts for landing gears of Airbus A350 XWB planes*. 2016; Available from: http://www.kobelco.co.jp/english/releases/1195041_15581.html.
7. Alec. *China showcases large 3D printed metal frames for new generation of military aircraft*. 2015; Available from: http://www.3ders.org/articles/20150717-china-showcases-large-3d-printed-metal-frames-for-new-generation-of-military-aircraft.html.
8. Hu, D. and R. Kovacevic, *Sensing, modeling and control for laser-based additive manufacturing.* International Journal of Machine Tools and Manufacture, 2003. **43**(1): p. 51-60.

9. Iravani-Tabrizipour, M. and E. Toyserkani, *An image-based feature tracking algorithm for real-time measurement of clad height.* Machine Vision and Applications, 2007. **18**(6): p. 343-354.
10. Toyserkani, E. and A. Khajepour, *A mechatronics approach to laser powder deposition process.* Mechatronics, 2006. **16**(10): p. 631-641.
11. Bi, G., et al., *Identification and qualification of temperature signal for monitoring and control in laser cladding.* Optics and lasers in engineering, 2006. **44**(12): p. 1348-1359.
12. Bi, G., et al., *Characterization of the process control for the direct laser metallic powder deposition.* Surface and Coatings Technology, 2006. **201**(6): p. 2676-2683.
13. Bi, G., et al., *Development and qualification of a novel laser-cladding head with integrated sensors.* International Journal of Machine Tools and Manufacture, 2007. **47**(3): p. 555-561.
14. Mazumder, J., et al., *Closed loop direct metal deposition: art to part.* Optics and Lasers in Engineering, 2000. **34**(4): p. 397-414.
15. Tang, L., et al., *Variable powder flow rate control in laser metal deposition processes.* Journal of Manufacturing Science and Engineering, 2008. **130**(4): p. 041016.
16. Doubenskaia, M., P. Bertrand, and I. Smurov, *Optical monitoring of Nd: YAG laser cladding.* Thin Solid Films, 2004. **453**: p. 477-485.
17. Hua, T., et al., *Research on molten pool temperature in the process of laser rapid forming.* journal of materials processing technology, 2008. **198**(1): p. 454-462.
18. Tan, H., et al., *Estimation of laser solid forming process based on temperature measurement.* Optics & Laser Technology, 2010. **42**(1): p. 47-54.
19. Heralić, A., A.-K. Christiansson, and B. Lennartson, *Height control of laser metal-wire deposition based on iterative learning control and 3D scanning.* Optics and lasers in engineering, 2012. **50**(9): p. 1230-1241.
20. Adeola Adediran, A.N., Lonnie Love, *An In-depth Review On the Scientific and Policy Issues Associated with Additive Manufacturing.* Journal of Science Policy & Governance, 2017. **11**(1).
21. Sciaky. *Advantages of Wire AM vs. Powder AM*. Available from: http://www.sciaky.com/additive-manufacturing/wire-am-vs-powder-am.
22. Adediran, A. and A. Oyedele, *Operational aspects and regulatory gaps in additive manufacturing*, in *Additive Manufacturing Handbook: Product Development for the Defense Industry*, V.V.V.a.D.L. Adedeji B. Badiru, Editor. 2017, Taylor and Francis/CRC Press, Boca Raton, FL. p. 7.
23. Kobryn, P.A.O., N.R.; Perkins, L.P.; Tiley, J.S. *Additive Manufacturing of Aerospace Alloys for Aircraft Structures*. in *Cost Effective Manufacture via Net Shape Processing. Meeting Proceedings RTO-MP-AVT-139, Paper 3*. 2006. Neuilly-sur-Seine, France: RTO.
24. Tapia, G. and A. Elwany, *A review on process monitoring and control in metal-based additive manufacturing.* Journal of Manufacturing Science and Engineering, 2014. **136**(6): p. 060801.
25. Abdullah, B., et al. *Monitoring of TIG welding using laser and diode illumination sources: A comparison study*. in *Electronic Design, 2008. ICED 2008. International Conference on*. 2008. IEEE.
26. Eriksson, I., et al., *New high-speed photography technique for observation of fluid flow in laser welding.* Optical Engineering, 2010. **49**(10): p. 100503-100503-3.
27. INOuE, K., *Image Processing for On-Line Detection of Welding Process (Report III): Improvement of Image Quality by Incorporation of Spectrum of Arc.* Transactions of JWRI, 1981. **10**(1): p. 13-18.
28. KIM, E., C. Allemand, and T. EAGAR, *Visible light emissions during gas tungsten arc welding and its application to weld image improvement.* micron, 1987. **500**(250): p. 100.
29. Ogawa, Y., *Visual Analysis of Welding Processes*. 2012: INTECH Open Access Publisher.

30. Photron, *Slow motion analysis of different welding techniques*, in *Arc welding Videos*. 2014, Photron Marketing.
31. Tadamalle, A., Y. Reddy, and E. Ramjee, *Influence of laser welding process parameters on weld pool geometry and duty cycle.* Advances in Production Engineering & Management, 2013. **8**(1): p. 52.